

Accepted Manuscript

Design, synthesis, anti-lung cancer activity, and chemosensitization of tumor-selective MCACs based on ROS-mediated JNK pathway activation and NF- κ B pathway inhibition

Liping Chen, Qian Li, Bixia Weng, Jiabing Wang, Yangyang Zhou, Dezhi Cheng, Thanchanok Sirirak, Peihong Qiu, Jianzhang Wu

PII: S0223-5234(18)30296-4

DOI: [10.1016/j.ejmech.2018.03.051](https://doi.org/10.1016/j.ejmech.2018.03.051)

Reference: EJMECH 10316

To appear in: *European Journal of Medicinal Chemistry*

Received Date: 22 December 2017

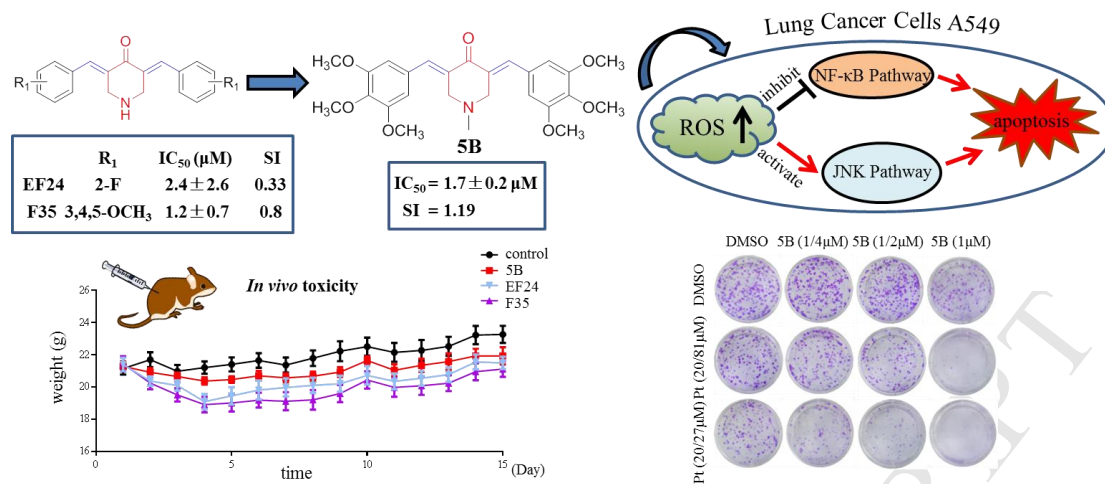
Revised Date: 28 February 2018

Accepted Date: 18 March 2018

Please cite this article as: L. Chen, Q. Li, B. Weng, J. Wang, Y. Zhou, D. Cheng, T. Sirirak, P. Qiu, J. Wu, Design, synthesis, anti-lung cancer activity, and chemosensitization of tumor-selective MCACs based on ROS-mediated JNK pathway activation and NF- κ B pathway inhibition, *European Journal of Medicinal Chemistry* (2018), doi: 10.1016/j.ejmech.2018.03.051.

This is a PDF file of an unedited manuscript that has been accepted for publication. As a service to our customers we are providing this early version of the manuscript. The manuscript will undergo copyediting, typesetting, and review of the resulting proof before it is published in its final form. Please note that during the production process errors may be discovered which could affect the content, and all legal disclaimers that apply to the journal pertain.





Design, Synthesis, anti-lung Cancer Activity, and Chemosensitization of Tumor-selective MCACs Based on ROS-mediated JNK Pathway Activation and NF- κ B Pathway Inhibition

Liping Chen^a, Qian Li^a, Bixia Weng^a, Jiabing Wang^a, Yangyang Zhou^{ab}, Dezhi Cheng^c,
Thanchanok Sirirak^d, Peihong Qiu^a, Jianzhang Wu^{a*}

^aChemical Biology Research Center, College of Pharmaceutical Sciences, Wenzhou Medical University, Wenzhou, Zhejiang 325035, China)

^bDepartment of Gastroenterology, The First Affiliated Hospital of Wenzhou Medical University, Wenzhou, Zhejiang 325035, China)

^cDepartment of Thoracic Surgery, The First Affiliated Hospital of Wenzhou Medical University, Wenzhou, Zhejiang 325035, China)

^dFaculty of Pharmaceutical Sciences, Burapha University, Bangsaen, Chonburi 20131, Thailand)

*Correspondence authors.

Address: Chemical Biology Research Center, College of Pharmaceutical Sciences, Wenzhou Medical University, Wenzhou, Zhejiang 325035, China. Tel./Tex: +86 577 86689984: (Jianzhang Wu).

wjzwzmu@163.com (Jianzhang Wu)

Abstract

EF24 and **F35** both were effective monocarbonyl curcumin analogs (MCACs) with excellent anti-tumor activity, however, drug defect such as toxicity may limit their further development. To get anti-lung cancer drugs with high efficiency, low toxicity and chemosensitization, a series of analogues based on EF24 and **F35** were designed and synthesized. A number of compounds were found to exhibit cytotoxic activities selectively towards lung cancer cells compared to normal cells. Among these compounds, **5B** was considered as an optimal anti-tumor agent for lung cancer cells with IC₅₀ values ranging from 1.0 to 1.7 μ M, selectivity index (SI, as a logarithm of a ratio of IC₅₀ value for normal and cancer cells) were all above 1.1, while the SI of EF24 and **F35** were less than 0.8. Consistent with selectivity *in vitro*, **5B** was observed to show lower toxicity in acute toxicity experiment than EF24 and **F35** respectively. Further, **5B** was found to exert anti-tumor effects through ROS-mediated activation of JNK pathway and inhibition of NF- κ B pathway. **5B** could significantly

enhance the sensitivity of A549 cells to cisplatin or 5-Fu. These findings suggested that **5B** was an effective and less toxic MCAC and provided a promising candidate for anti-tumor drugs.

Keywords: MCACs; Synthesis; Toxicity; Anti-tumor activities; Chemosensitization

1. Introduction

To date, lung cancer is one of the most threatening malignant tumors against human health[1,2]. There are 1800,000 new cases of lung cancer worldwide every year[3]. Due to the lack of valid methods for early diagnosis and unobvious symptoms of early lung cancer, most patients are found at an advanced stage and can not be treated by surgical removal, thus the main efficacious therapy is chemotherapy[4,5]. With the discovery of a variety of cancer-specific molecular biomarkers, personalized therapy for the tumor specific targets has gradually become a popular issue in the development of anti-lung cancer drugs[1,3]. Unfortunately, it is not just the frequent appearance of resistance concomitant with targeted therapies, but the higher budgets for targeted drugs that account for the limited use of targeted preparations[6,7]. In addition, not all driver mutations have been identified in lung cancer cells and matched with effective targeted drugs[8,9], leading to the classical cytotoxic drugs remain the first choice for patients ineffective in targeted therapies[10]. Whereas, the use of cytotoxic drugs such as cisplatin, paclitaxel are accompanied by side effects and chemoresistance[11-13], which may restrict drug dosage, impose the burden of disease and impair the level of patients' health-related quality of life. To change the current status of lung cancer treatment, less toxic and effective compounds as well as chemosensitizers therefore have received increasing attention.

Natural products without obvious toxicity have been an important source of new drug discovery and inspired the drug development having novel scaffolds[14]. Curcumin, extracted from the *Curcuma longa* with outstanding pharmacological activities[15,16], has attracted a lot of attention. Unfortunately, no successful progress has been made in the curcumin-related clinical trials, which could partly be explained by its instability as well as pharmacokinetic deficiencies caused by unstable β -diketone structure[16,17]. As a consequence, many scholars have focused on the study of altering curcumin-unstable β -diketone to monocarbonyl curcumin analogues (MCACs), which have been reported to retain or raise the biological activities with improvement of the pharmacokinetics[17-20]. Among the derivatives, EF24 is a hot-studied MCAC, found to have superior anti-tumor activities[21]. Nevertheless,

further clinical development into an applicable drug candidate may be impeded by its toxicity[22,23]. Similarly, a series of MCACs with great pharmacological activities have been designed and synthesized in our previous study[24-27]. For example, **F35**, **F36**, as EF24 analogues with structure of multiple methoxys on benzene ring, found to exhibit preferable anti-inflammatory activities by inhibiting the NF- κ B pathway. With the research deep-going, **F35** was also identified as a good anti-tumor compound. However, like EF24, **F35** exhibited toxicity to a certain degree *in vitro* and *in vivo*.

Given that multi-methoxy phenyl was a key functional group in many natural products with excellent anti-tumor activities, including piperlongumine, combretastatin-A4 and terameprocol[28-30]. It has been reported that N-substituted curcumin analogues on the piperidone moiety showed limited toxicity towards normal cells[31,32]. Thus, for the purpose of finding efficient and low-toxicity anti-lung cancer compounds, a series of piperid-4-one-containing MCACs bearing the structure of multi-methoxy phenyl (3,4,5-OCH₃ or 3,4-OCH₃) were designed and synthesized based on the lead compounds of EF24, **F35** and **F36**. Among these compounds, **5B**, as an optimal compound with higher efficiency and lower toxicity superior to EF24 and **F35**, was selected for the study of anti-tumor mechanism and found to exert anti-tumor effects via ROS-mediated JNK and NF- κ B pathways preliminarily.

2. Results and discussion

2.1 Design and synthesis

In the present study, we synthesized a series of MCACs. Piperidone embedded in two benzene rings conjugated with flanking C=C bonds was used to displace the central keto-enol curcuminoid moiety. MCACs with 3,4,5-trimethoxyl or 3,4-dimethoxyl substituents on both benzene rings were designed and synthesized (Figure 1A). Generally, MCACs (**F35**, **F36**) can be easily achieved by aldol condensation reaction between 4-piperidinone and aldehydes, and MCACs (**5B-13B**) with N-substitution with different groups (methyl, ethyl, n-propyl, propionyl, formyl propionyloxy, 2-fluorobenzoyl, isobutyryl) on the piperidone moiety can be synthesized by **F35**, **F36** and various alkyl halide or acyl chloride, respectively (Figure 1B). The structures of MCACs were shown in Figure 1C, and confirmed by nuclear magnetic resonance (¹H-NMR) spectroscopy and Liquid Chromatography-Mass Spectrometry (LC-MS)

analysis. The color, melting point, LC-MS and $^1\text{H-NMR}$ spectrum of compounds were presented in the chemical section.

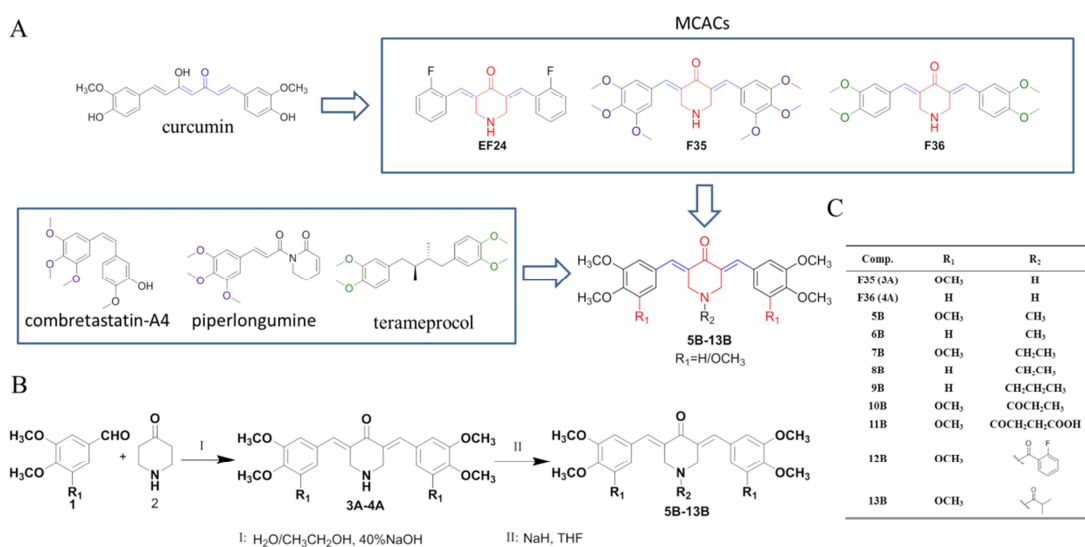


Figure 1. Design, synthesis and structures of MCACs. (A) Design of MCACs. (B) Synthetic pathway to MCACs. Reagents and conditions: (I) $\text{H}_2\text{O}/\text{CH}_3\text{CH}_2\text{OH}$, 40%NaOH, room temperature; (II) NaH, THF, 0 °C. (C) Chemical structures of synthesized MCACs.

2.2 The inhibition effects to cell viability

All compounds were evaluated by measuring the anti-viability activities to human lung cancer cells H460, A549, H1650 and H1975 using MTT assay[33]. The half inhibitory concentration (IC_{50}) of these compounds were measured and listed in Table 1. Except that compound **11B** showed low activity, other compounds induced a significant loss of cell viability on the four types of cancer cells, whose IC_{50} reached approximately 5.0 μM . In recent years, our research group has been engaged in MCACs medicinal chemistry research and reviewed on the pharmacological activities of 607 MCACs reported in the literature. Among them, many MCACs had good anti-tumor effects, namely, the IC_{50} upon cancer cells generally reached the level of 1-5 μM except for some of them less than 1 μM . The results showed that the tested compounds demonstrated a significant anti-viability effects against H460 cells and most of them with the IC_{50} were less than 5 μM , especially **5B**, **12B** and **13B**, whose IC_{50} were within 2.0 μM ; The same results could be observed in A549 cells, especially compounds **10B**, **12B** and **13B**, whose IC_{50} had reached 0.8 μM . Similarly, in the other two cell lines, the majority of tested substances also showed excellent inhibitory efficacy, which were just as effective as EF24, **F35**, and better than curcumin. Therefore, the anti-tumor activities of these compounds designed in this essay had

generally reached a good level. Given the above, the existence of these structures including EF24, **F35** basic skeleton and multi-methoxy phenyl (3,4,5-OCH₃ or 3,4-OCH₃) that may contributed to good activities.

Table 1. Cytotoxicity and selectivity index (SI) of compounds on various human lung cancer cells and normal cells

Compound	IC ₅₀ ^a (μM) for cell lines/SI ^b				
	H460	A549	H1650	H1975	HL7702
F35 (3A)	1.5±0.6/0.70	1.2±0.7/0.80	4.2±3.1/0.26	4.0±3.5/0.28	7.6±0.9
F36 (4A)	6.4±1.8/0.37	2.9±3.1/0.72	16.7±7.4/-0.04	10.3±5.9/0.17	15.1±7.2
5B	1.0±0.3/1.42	1.7±0.2/1.19	1.5±0.1/1.25	1.0±0.6/1.42	26.4±3.3
6B	3.1±1.9/0.77	1.3±0.9/1.15	9.0±2.9/0.31	6.6±6.8/0.44	18.2±0.9
7B	4.9±6.0/0.42	4.2±2.8/0.48	8.2±2.3/0.19	6.5±0.1/0.29	12.8±2.8
8B	3.6±1.8/0.43	3.6±4.2/0.43	12.0±3.6/-0.09	8.5±2.6/0.06	9.8±0.1
9B	4.1±3.8/0.71	4.2±1.8/0.70	16.0±12.2/0.12	11.2±5.9/0.27	21.0±0.9
10B	2.7±1.8/0.19	0.8±0.9/0.72	4.4±1.2/-0.02	1.7±0.5/0.39	4.2±0.1
11B	>60 ^c /nc ^d	17.9±15.5/nc ^d	>60 ^c /nc ^d	>60 ^c /nc ^d	>60 ^c
12B	1.5±0.7/0.47	0.7±0.8/0.80	1.9±1.0/0.36	1.4±0.2/0.50	4.4±1.6
13B	2.0±0.2/0.79	0.8±0.9/1.18	10.8±0.9/0.05	1.9±0.2/0.81	12.2±6.7
BAY	16.8±6.9/nc ^d	15.9±3.1/nc ^d	53.2±5.9/nc ^d	32.0±16.9/nc ^d	>60 ^c
BMS345541	2.8±2.6/0.74	8.6±0.8/0.25	9.3±1.7/0.22	8.0±2.5/0.28	15.3±4.8
Curcumin	8.5±1.1/-0.07	6.8±0.2/0.02	20.5±5.7/-0.45	1.4±0.3/0.71	7.2±0.6
EF24	1.2±0.9/0.63	2.4±2.6/0.33	1.7±0.4/0.48	1.3±0.1/0.59	5.1±1.6

^a IC₅₀ was the concentration of a drug that reduced cell viability by 50% relative to the untreated control.

^b SI has been calculated as a logarithm of a ratio of IC₅₀ value for normal cells (HL7702) and the IC₅₀ value for cancer cells (H460, A549, H1650 and H1975).

^c The maximum use of the compound concentration.

^d nc (not calculated) – the SI could not be calculated because of lack of the IC₅₀ value for normal/cancer cells.

2.3 *In vitro* and *vivo* toxicity

For the purpose to select efficient and hypotoxic anti-tumor compounds, the cytotoxicity of tested substances were investigated further on normal human liver

cells HL7702. The results were showed in Table 1. It is found that most compounds showed higher IC_{50} of HL7702 than the cancer cells, indicating selectivity of HL7702 towards cancer cells at different extent, while the lead compound curcumin induced no significant selectivity. In particular, compound **5B** was more cytotoxic in four types of cancer cells with selectivity index (SI, as a logarithm of a ratio of IC_{50} value for normal and cancer cells) values in the range of 1.1-1.5. More delightfully, **5B** had the advantage of being more selective than EF24 and **F35**, whose SI were within 0.8. Thus, it was speculated that the raised selectivity of **5B**, **13B** and others, even higher than EF24, **F35** and **F36**, may be related to N-substitutions.

As highlighted above, the advantage of **5B** was its high activity and low hepatotoxicity *in vitro*. Further, acute toxicity experiment was carried out to determine whether **5B** was safer than EF24 and **F35** *in vivo*[34]. The study was performed on mice by recording the changes in body weight. It was shown in Figure 2 that the effect of **5B** on body weight was lower than EF24 and **F35** respectively, regardless of whether it was administered intraperitoneally or intragastrically, which were in agreement with *in vitro* findings, although there was no denying that **5B** showed a certain degree of toxicity *in vivo*. These findings suggested that as EF24 and **F35** derivatives, **5B** performed better selectivity *in vitro* and lower toxicity *in vivo*.

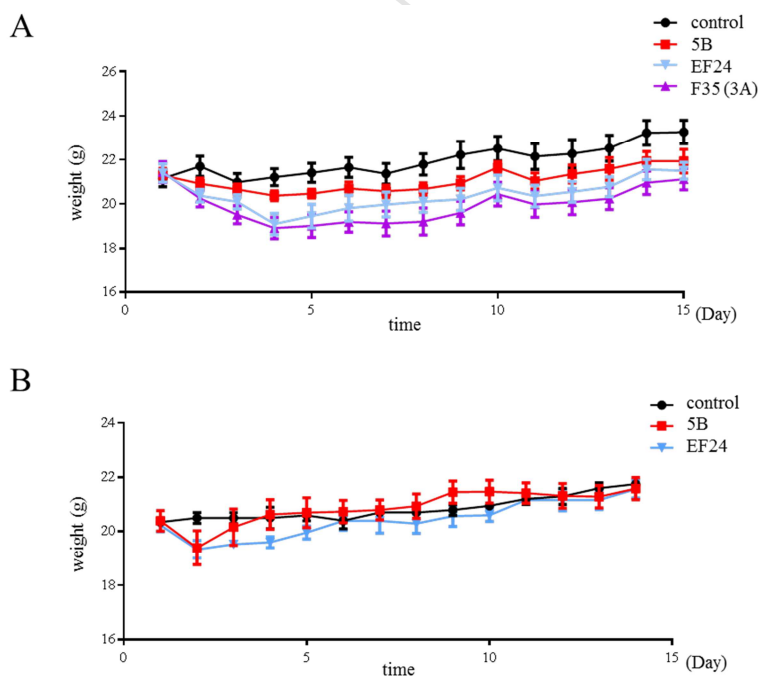


Figure 2. **5B** showed less toxicity than EF24 and **F35** respectively *in vivo*. (A) Changes in body weight of C57BL/6 mice administered by intraperitoneal injection with vehicle (6% castor oil), **5B**, EF24, **F35**. The weight of the mice were observed for 15 days. (B) Changes in body weight of C57BL/6 mice treated by lavage with vehicle (0.5% CMC-Na), **5B**, EF24 were monitored for 14 days.

2.4 **5B** induced cell cycle arrest and apoptosis in A549 cells

To study the potential mechanistic pathways responsible for the inhibitory effects, the changes in cell cycle distribution and apoptosis in response to **5B** were analyzed. As shown in Figure 3, A549 cells treated with **5B** clearly induced a dose-dependent arrest of G2/M phase, while the cell proportion in G2/M phase induced by positive control BMS345541 was lower than **5B** with the concentration of 5 μM . The results in Figure 4A-C indicated that **5B** induced obvious cell apoptosis in a dose-dependent manner. Compared to **5B** (10 μM) treated cells, BMS345541 (20 μM) induced less percentage of apoptosis. To determine the role of proapoptotic effects in **5B**-mediated cells, apoptosis-related proteins were also studied. As depicted in Figure 4D-E, the cleavage of poly (ADP-ribose) polymerase (PARP), an apoptosis marker, by activated caspase 3 was observed in a dose-dependent increase after 24 h treatment. Similarly, **5B**-treated groups showed a significant increase in the level of Bax, a Bcl-2 family protein. All results indicated that **5B** had the capacity of anti-tumor activities by arresting cell cycle and inducing apoptosis.

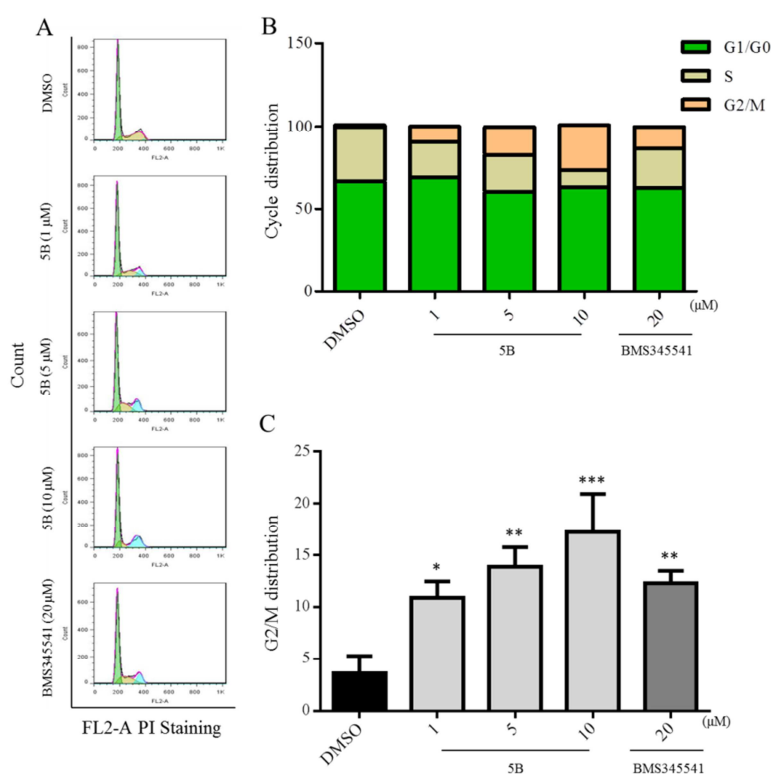


Figure 3. **5B** induced cell cycle arrest of G2/M phase in A549 cells. (A) Flow cytometry was performed to study the effects of **5B** in cell cycle. A549 cells were treated with **5B** (1 μM , 5 μM and 10 μM) for 10 h, BMS345541 (20 μM) was used as positive control. (B) The frequency distribution bar chart of G1/G0, S, G2/M. (C) Histograms displayed DNA content of G2/M. *, $p <$

0.05; **, $p < 0.01$; ***, $p < 0.001$, vs DMSO.

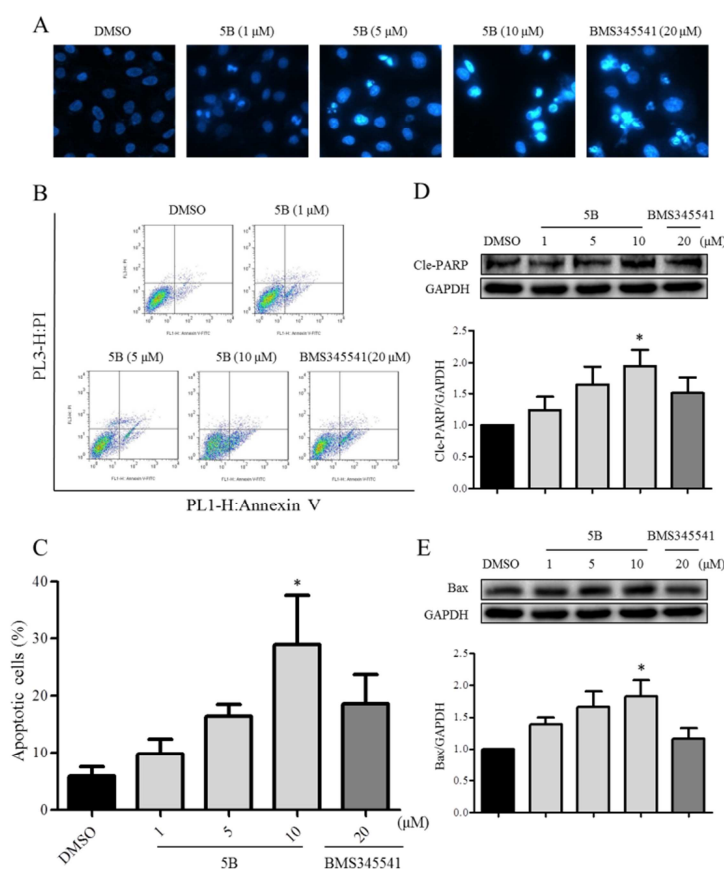


Figure 4. 5B induced apoptosis in A549 cells. (A-B) 5B induced increased apoptotic morphology and apoptotic ratio respectively. A549 cells were treated with 5B (1 μM, 5 μM and 10 μM) or BMS345541 (20 μM) for 24 h. (C) The proportion of apoptotic cells from (B) was calculated after Annexin V/PI double staining. (D-E) Western blot was performed to assess the expression of apoptosis-related proteins Cle-PARP and Bax after 5B or BMS345541 treatment for 24 h. *, $p < 0.05$, vs DMSO.

2.5 5B induced the generation of ROS

Reactive Oxygen Species (ROS) was recognized as a key factor in many cellular signaling events, including cell apoptosis and necrosis[35-37]. In cancer cells, apoptosis was induced at a higher level of ROS, therefore, in search of ROS-inducing compounds to target cancer has been considered as a potential strategy[35-37]. Curcumin derivatives including EF24 were reported to exhibit anti-tumor activities by generating ROS[38-40]. Consequently, the level of intracellular ROS was monitored using a ROS-sensitive fluorogenic dye (dichlorodihydrofluorescein diacetate, DCF-DA) by flow cytometry to investigate whether 5B could generate ROS in A549 cells. Imaging analysis revealed that 5B strongly generated ROS in the range of 0 to 9 h, but slightly decreased at the time of 12 h (Figure 5A). In addition, ROS generation

was observed dose-dependently after treating the cells with **5B** (1 μM , 5 μM and 10 μM) for 9 h (Figure 5B). Further, ROS inhibitor N-acetyl cysteine (NAC) was used to identify the role of ROS in mediating **5B**'s anti-tumor effects. As shown in Figure 5C, the generation of ROS was greatly attenuated when cells were pre-treated with NAC for 1 h. And as expected, apoptosis induced by **5B** was almost completely reversed by NAC pre-treatment (Figure 5D). These results suggested that ROS production mediated **5B**-activated apoptosis.

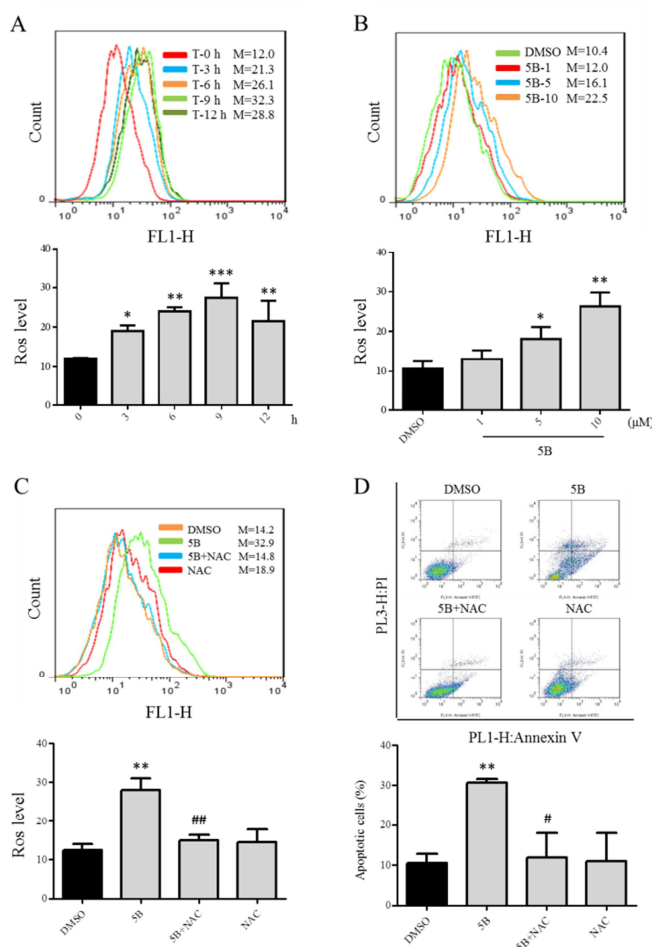


Figure 5. **5B** induced apoptosis in A549 cells was dependent on the generation of ROS. (A-B) ROS generation was measured in cells following exposure to **5B** (10 μM) for various time periods and various concentrations for 9 h. (C) A549 cells were pre-treated with or without NAC (5 mM) for 1 h before exposure to **5B** (10 μM) for 9 h. ROS production was measured by flow cytometry. (D) Effects of ROS decrease on cell apoptosis. A549 cells were pre-treated with or without NAC (5 mM) for 1 h before exposure to **5B** (10 μM) for 24 h. Percentage of cell apoptosis was determined by flow cytometry. *, $p < 0.05$; **, $p < 0.01$; ***, $p < 0.001$, vs DMSO. #, $p < 0.05$; ##, $p < 0.01$, vs **5B**.

2.6 The activation effects of **5B** on JNK pathway

It has been reported that in response to ROS, JNK signaling pathway was often

activated, ultimately leading to apoptosis, which was also found in curcumin analogs including EF24[41,42]. Thus, the effects of **5B** on the JNK pathway and the relationship between ROS and JNK were examined. Western blot analysis revealed that treatment with **5B** at a set four time points increased the phosphorylation of JNK1/2, and treatment for 6 h multiplied the phosphorylation of JNK1/2 in a dose-dependent manner (Figure 6A-B). Subsequently, to make sure if **5B** induced apoptosis through activating JNK pathway, its specific JNK inhibitor namely SP600125 was applied to this study. It was not difficult to find that **5B**-induced JNK phosphorylation and apoptosis were effectively abolished by SP600125 (Figure 6C, 6E and 6F). Furthermore, pre-treatment with NAC for 1 h downregulated the phosphorylation of JNK1/2 and attenuated **5B**-induced apoptosis (Figure 6D and 5D). These results suggested that the activated JNK pathway induced by **5B** was at least partly exerted in A549 cells and promoted apoptosis, and the multiplied ROS levels mediated the enhanced JNK pathway.

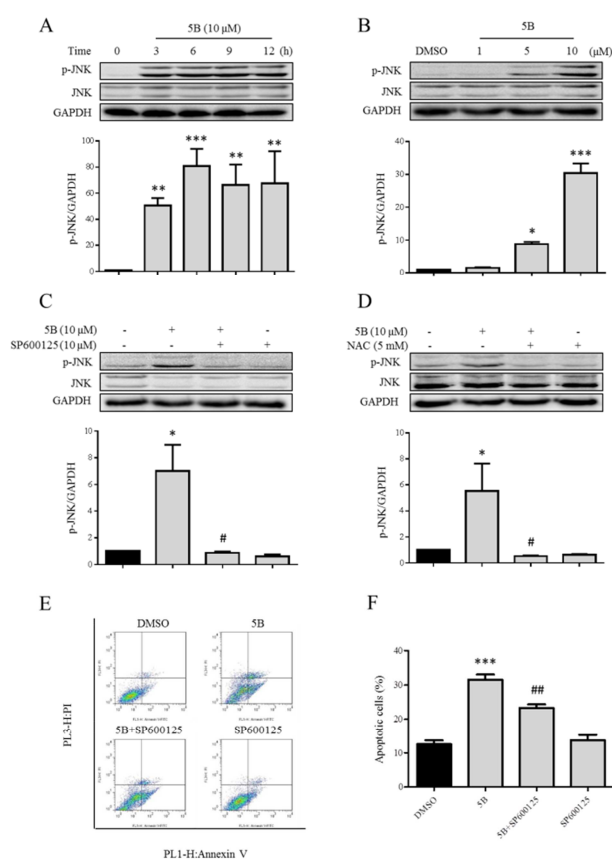


Figure 6. **5B** induced apoptosis in A549 cells via ROS-mediated JNK pathway. (A-B) The expression of p-JNK was detected by western blot. A549 cells were exposed to **5B** (10 μM) for various time periods and various concentrations for 6 h. GAPDH was used as internal control. (C-D) A549 cells were pre-treated with or without SP600125 (10 μM) and NAC (5 mM) for 1 h before exposure to **5B** (10 μM) for 6 h respectively. Western blot analysis was performed to assess

the expression of p-JNK. (E) Blocking of JNK pathway abolished the cell apoptosis induced by **5B**. A549 cells were pre-treated with or without SP600125 (10 μ M) for 1 h before exposure to **5B** (10 μ M) for 24 h. Induction of apoptosis was determined by flow cytometry. (F) The percentage of apoptotic cells from (E) was calculated. *, $p < 0.05$; **, $p < 0.01$; ***, $p < 0.001$, vs DMSO. #, $p < 0.05$; ##, $p < 0.01$, vs **5B**.

2.7 The inhibition effects of **5B** on NF- κ B pathway

The abnormal NF- κ B activation has been reported to correlate with the occurrence and development of lung cancer[43,44]. Namely, under normal circumstances, NF- κ B is connected with its inhibitor I κ B α in a non-active state. In certain cases of lung cancer, IKK (inhibitor kappa B kinase) is being continuously phosphorylated, that is, in a high activity state. Activated IKK introduces phosphorylation of its substrate I κ B α . Then phosphorylated I κ B α dissociates from the NF- κ B. Soon afterwards NF- κ B enters the nucleus and starts regulating anti-tumor apoptotic protein Bcl-2 expression, promoting tumor formation. It was known from previous studies that **F35** and EF24 inhibited NF- κ B signaling pathway playing anti-inflammatory effects[24,45]. Herein, we performed western blot analysis to determine the effects of TNF α -induced I κ B α degradation on A549 via compound **5B** (1 μ M, 5 μ M and 10 μ M), BMS345541 was selected as control. As shown in Figure 7A, TNF α -induced I κ B α degradation was inhibited when stimulated by TNF α for 15 min after 1 h of **5B** action. Additionally, the inhibitory effect induced by **5B** was restrained in plasmid IKK β transfected cells relative to mock-vehicle group (Figure 7C), all of which suggested that **5B**-induced apoptosis was mediated by NF- κ B pathway. Western blot was used to confirm the success of plasmid IKK β transfection (Figure 7B).

Reports showed that NF- κ B inhibition was associated with ROS generation, which played the important role in anti-tumor[46]. Therefore, we further confirmed whether ROS production stimulated **5B**-induced apoptosis by inhibiting NF- κ B pathway. Interestingly, pre-treatment with NAC for 1 h reduced the expression of I κ B α (Figure 7D), indicating **5B**-induced NF- κ B inhibition was activated by ROS inhibitor, ROS generation had created a significant inhibitory activity on the NF- κ B pathway. Given the above, ROS production triggered **5B**-induced apoptosis via activating JNK pathway and inhibiting NF- κ B pathway, more importantly, there were still few reports on the anti-tumor effects of curcumin analogues via ROS-mediated JNK and NF- κ B pathways.

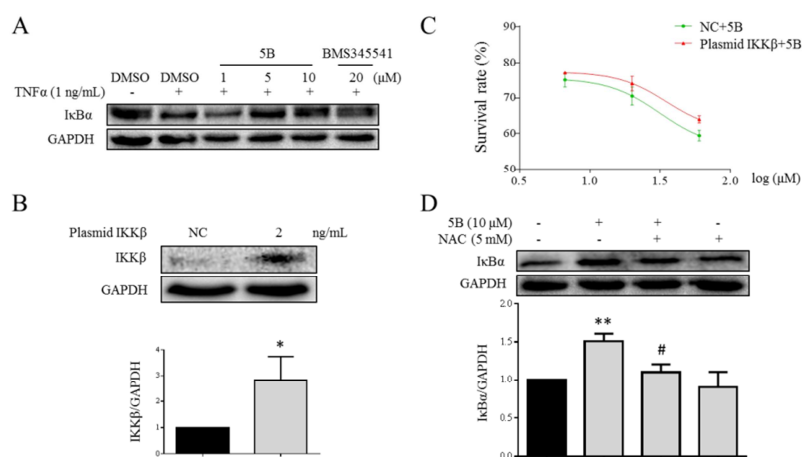


Figure 7. **5B** induced apoptosis in A549 cells via ROS-mediated NF- κ B pathway. (A) A549 cells were pre-incubated with **5B** of different concentrations or BMS345541 (20 μ M) for 1 h before the addition of TNF α (1 ng/mL) for 15 min. The expression of I κ B α was detected by western blot. GAPDH was used as internal control. (B) A549 cells were infected with plasmid IKK β (2 ng/mL) or empty vector. The transfection effect was confirmed by western blot. (C) A549 cells transfected with plasmid IKK β or empty vector were treated with **5B** (60, 20, 6.67 μ M) for 24 h. The cell vitality underlying Ad10's action was determined using MTT assay (D) The effects of ROS inhibitor on I κ B α degradation. A549 cells were pretreated with or without NAC (5 mM) for 1 h before exposure to **5B** (10 μ M) for 1 h. I κ B α level was analyzed by western blot. GAPDH was used as internal control. **, $p < 0.01$, vs DMSO. #, $p < 0.05$, vs **5B**.

2.8 The chemosensitization effects of **5B**

Cisplatin is a first-line anti-lung cancer chemotherapeutic drug, whose use is limited due to its dose-related side effects[47]. Searching for compounds combined with cisplatin to reduce the amount of cisplatin and improve the efficacy has bright prospects. It has been reported that NF- κ B activation was a mechanism contributing to tumor resistance to cisplatin[12,13], which prompted us to investigate that whether **5B**, as a NF- κ B inhibitor, had sensitizing effects with cisplatin. As consistent with previous reports, NF- κ B could be activated by cisplatin (Figure 8A). In addition, cisplatin-induced IKK phosphorylation could be inhibited via **5B** in a dose-dependent manner (Figure 8B). Ulteriorly, clonogenic assay verified that the combination of **5B** and cisplatin could significantly inhibit the formation of colony and increase cisplatin sensitivity (Figure 8C). Similarly, the combination with anti-lung cancer drug 5-Fu also existed unexpected combined effects (Figure 8C). Undeniably, high-efficient and low-toxic compound **5B** with capacity of combination with anti-lung cancer drugs deserved to be further studied.

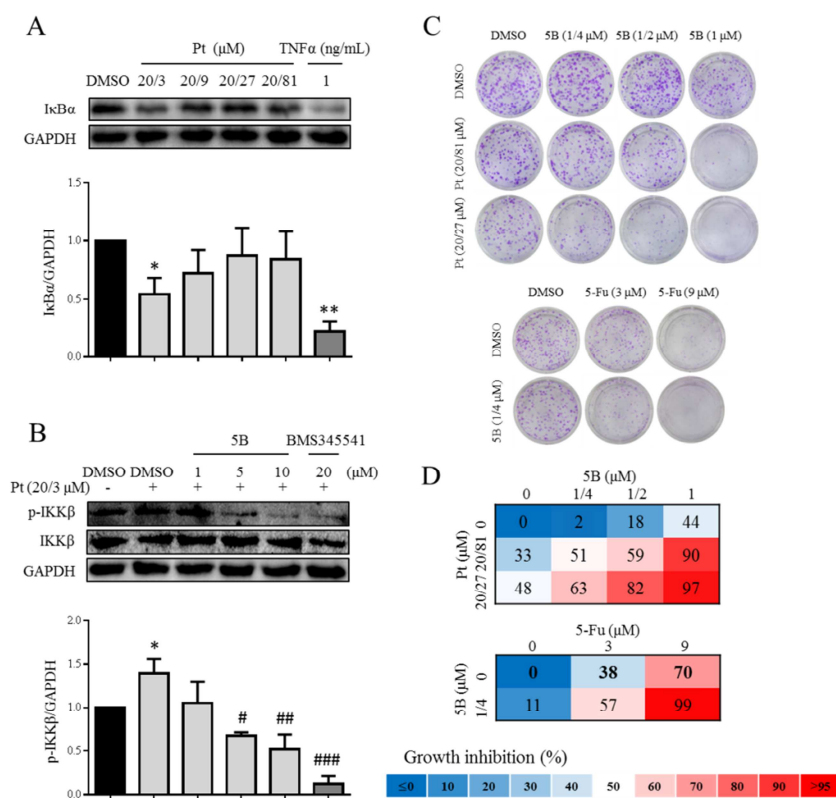


Figure 8. The chemosensitization effects of **5B** with cisplatin (Pt) and 5-Fu in A549 cells. (A) IκBα level was measured in cells following exposure to Pt of various concentrations for 24 h and TNFα (1 ng/mL) for 15 min. GAPDH was used as internal control of western blot analysis. (B) A549 cells were pretreated with **5B** (1 μM, 5 μM and 10 μM) or BMS345541 (20 μM) for 1 h before exposure to Pt (20/3 μM) for 24 h. Western blot analysis was performed to assess the expression of p-IKKβ. (C) Clonogenic assay of A549 cells treated with increasing concentrations of **5B**, Pt, or their combination as well as **5B**, 5-Fu or their combination as indicated. (D) Percent inhibition at each concentration of the drugs from (C) was calculated and represented as the percent of control. *, $p < 0.05$; **, $p < 0.01$, vs DMSO. #, $p < 0.05$; ###, $p < 0.01$; ####, $p < 0.001$, vs (DMSO + Pt).

3. Conclusion

Lung cancer remains the main cause of death worldwide and there still lacks anti-lung cancer drugs without obvious side effects. In this study, a series of MCACs with promising anti-tumor activities have been designed and synthesized based on EF24 and **F35** motif. Notably, synthesized compounds generally exhibited better selectivity than curcumin, several of whom proved to display more prominent selectivity in relation to reference compounds, EF24, **F35** and **F36**. Among them, **5B** was considered as a promising anti-tumor agent in selectively killing cancer and normal cells with greatly enhanced inhibitory potential. Given that all compounds were

designed and featured with multi-methoxy group as well as nitrogen substituents, which may be associated with changes in activity and toxicity respectively. More importantly, this assumption needs to be further fully confirmed. Even more gratifying is that, preferred compound **5B** showed less toxicity *in vivo* than EF24 and **F35**, indicating that **5B** had a considerable potential in lung cancer research.

Thereupon, molecular mechanism of **5B** was elaborated and found to induce cell cycle arrest in G2/M phase. In addition, **5B** subsequently induced apoptosis by activating JNK and inhibiting NF- κ B signaling pathways respectively, both of which were associated with the generation of ROS. Nevertheless, there were few reports on anti-tumor activities of MCACs via ROS-mediated JNK and NF- κ B pathways. Meanwhile, **5B** was proved to have combined effects with cisplatin or 5-Fu, which, to a certain extent, reducing the dose of cisplatin or 5-Fu for therapy. Conceivably, the discovery of **5B** with high efficiency, low toxicity and chemosensitization highlighted its potential therapeutic applications in lung cancer treatment.

4. Experimental section

4.1 Synthesis

4.1.1 Chemistry

All reagents were obtained from commercial suppliers Sigma-Aldrich and Aladdin. The reaction processes were monitored by thin-layer chromatography via using silica gel GF254, and the chromatograms were performed with silica gel (200-300 mesh) and visualized under UV light at 254 or 365 nm. Final compounds of melting points were determined on open capillary tubes on a Fisher-Johns melting apparatus. Mass spectrometry analyses were determined on an Agilent 1100 LC-MS (Agilent, Palo Alto, CA, USA). ^1H spectral data were recorded on 600 MHz spectrometer (Bruker Corporation, Switzerland). The chemical data of compounds were presented as follows:

3,5-bis((E)-3,4,5-trimethoxybenzylidene)piperidin-4-one (3A): yellow powder, 68.8% yield, mp 191.7-194.1 °C (Lit[24] 193.7-194.0 °C). $^1\text{H-NMR}$ (CDCl_3) δ : 7.751 (s, 2H, H- α ×2), 6.643 (s, 4H, H-2, H-6×2), 4.220 (d, $J=1.2\text{Hz}$, 4H, CH_2 ×2), 3.912 (d, $J=5.4\text{Hz}$, 18H, 3-OCH₃, 4-OCH₃, 5-OCH₃×2). LC-MS m/z : 456.20, calcd for $\text{C}_{25}\text{H}_{29}\text{NO}_7$: 455.19.

3,5-bis((E)-3,4-dimethoxybenzylidene)piperidin-4-one (4A): yellow powder, 78.7% yield, mp 159.2-161.2 °C (Lit[24] 162.2-165.4 °C). $^1\text{H-NMR}$ (CDCl_3) δ : 7.758 (s, 2H, H- α ×2), 7.008 (d, $J=8.4\text{Hz}$, 2H, H-2×2), 6.908-6.933 (m, 4H, H-5, H-6×2), 4.191 (s, 4H, CH_2 ×2), 3.895-3.947 (m, 12H, 4-OCH₃, 3-OCH₃×2). LC-MS m/z : 396.29, calcd for $\text{C}_{23}\text{H}_{25}\text{NO}_5$: 395.17.

1-methyl-3,5-bis((E)-3,4,5-trimethoxybenzylidene)piperidin-4-one (5B): yellow powder, 45.9%

yield, mp 143.7-146.0 °C Lit[48]. ¹H-NMR (CDCl₃) δ: 7.768 (s, 2H, H-α×2), 6.647 (s, 4H, H-2, H-6×2), 3.917 (d, *J*=5.4Hz, 18H, 3-OCH₃, 4-OCH₃, 5-OCH₃×2), 3.818 (s, 4H, CH₂×2), 2.497 (s, 3H, CH₃). LC-MS *m/z*: 470.29, calcd for C₂₈H₃₁NO₇: 469.21.

3,5-bis((E)-3,4-dimethoxybenzylidene)-1-methylpiperidin-4-one (6B): yellow powder, 59.7% yield, mp 158.8-161.8 °C (Lit[24] 157.3-159.4 °C). ¹H-NMR (CDCl₃) δ: 7.784 (s, 2H, H-α×2), 7.029 (d, *J*=8.4Hz, 2H, H-6×2), 6.949 (t, *J*=19.8Hz, 4H, H-2, H-5×2), 3.940 (d, *J*=9.0Hz, 12H, 3-OCH₃, 4-OCH₃×2), 3.808 (s, 4H, CH₂×2), 2.506 (s, 3H, CH₃). LC-MS *m/z*: 410.26, calcd for C₂₄H₂₇NO₅: 409.19.

1-ethyl-3,5-bis((E)-3,4,5-trimethoxybenzylidene)piperidin-4-one (7B): yellow powder, 65.9% yield, mp 150.3-153.2 °C Lit[48]. ¹H-NMR(CDCl₃) δ: 7.762 (s, 2H, H-α×2), 6.642 (s, 4H, H-2, H-6×2), 3.892 (t, *J*=17.4Hz, 22H, 3-OCH₃, 4-OCH₃, 5-OCH₃×2, CH₂×2), 2.634 (d, *J*=7.2Hz, 2H, CH₂), 1.089 (t, *J*=13.8Hz, 3H, CH₃). LC-MS *m/z*: 484.45, calcd for C₂₇H₃₃NO₇: 483.23.

3,5-bis((E)-3,4-dimethoxybenzylidene)-1-ethylpiperidin-4-one (8B): yellow powder, 57.3% yield, mp 186.1-187.4 °C (Lit[24] 188.7-190.8 °C). ¹H-NMR (CDCl₃) δ: 7.799 (s, 2H, H-α×2), 7.035-7.052 (m, 2H, H-2×2), 6.977 (d, *J*=1.8Hz, 2H, H-6×2), 6.947 (d, *J*=8.4Hz, 2H, H-5×2), 3.944 (t, *J*=10.2Hz, 12H, 3-OCH₃, 4-OCH₃×2), 3.878 (s, 4H, CH₂×2), 2.637-2.673 (m, 2H, CH₂), 1.107 (t, *J*=14.4Hz, 3H, CH₃). LC-MS *m/z*: 424.35, calcd for C₂₅H₂₉NO₅: 423.20.

3,5-bis((E)-3,4-dimethoxybenzylidene)-4-methylene-1-propylpiperidine (9B): yellow powder, 58.6% yield, mp 166.5-167.6 °C (Lit[24] 162.7-165.2 °C). ¹H-NMR(CDCl₃) δ: 7.769 (s, 2H, H-α×2), 7.022 (dd, *J*=1.8, 8.4Hz, 2H, H-6×2), 6.955 (d, *J*=1.2Hz, 2H, H-2×2), 6.926 (d, *J*=8.4Hz, 2H, H-5×2), 3.952 (s, 6H, 3-OCH₃×2), 3.924 (s, 6H, 4-OCH₃×2), 3.854 (s, 4H, CH₂×2), 2.520 (t, *J*=18.4Hz, 2H, CH₂), 1.502-1.463 (m, 2H, CH₂), 0.884 (t, *J*=7.2Hz, 3H, CH₃). LC-MS *m/z*: 438.25, calcd for C₂₆H₃₁NO₅: 437.22.

1-propionyl-3,5-bis((E)-3,4,5-trimethoxybenzylidene)piperidin-4-one (10B): yellow powder, 55.6% yield, mp 165.9-167.9 °C. ¹H-NMR (CDCl₃) δ: 7.800 (d, *J*=33.0Hz, 2H, H-α×2), 6.752 (s, 2H, H-2×2), 6.625 (s, 2H, H-6×2), 4.971 (s, 2H, CH₂), 4.774 (s, 2H, CH₂), 3.937 (d, *J*=13.2 Hz, 18H, 3-OCH₃, 4-OCH₃, 5-OCH₃×2), 2.271-2.234 (m, 2H, CH₂), 1.073 (t, *J*=15.0Hz, 3H, CH₃). LC-MS *m/z*: 512.25, calcd for C₂₈H₃₃NO₈: 511.22.

4-oxo-4-(4-oxo-3,5-bis((E)-3,4,5-trimethoxybenzylidene)piperidin-1-yl)butanoic acid (11B): yellow powder, 60.4% yield, mp 171.5-174.4 °C. ¹H-NMR (CDCl₃) δ: 7.689 (d, *J*=18.6Hz, 2H, H-α×2), 6.871 (d, *J*=9.0Hz, 4H, H-2, H-6×2), 4.988 (d, *J*=22.8Hz, 4H, CH₂×2), 3.909 (d, *J*=6.0Hz, 12H, 3-OCH₃, 5-OCH₃×2), 3.780 (d, *J*=16.2Hz, 6H, 4-OCH₃×2), 2.579-2.600 (m, 2H, CH₂), 2.480-2.527 (m, 2H, CH₂). LC-MS *m/z*: 556.36, calcd for C₂₉H₃₃NO₁₀: 555.21.

1-(2-fluorobenzoyl)-3,5-bis((E)-3,4,5-trimethoxybenzylidene)piperidin-4-one (12B): yellow powder, 65.6% yield, mp 175.6-176.2 °C. ¹H-NMR (CDCl₃) δ: 7.762 (s, 1H, H-6'), 7.620 (s, 1H, H-4'), 7.331-7.369 (m, 1H, H-α), 7.263-7.290 (m, 1H, H-α'), 7.077-7.104 (m, 1H, H-5'), 7.304 (t, *J*=18.6Hz, 1H, H-3'), 6.951 (s, 2H, H-2×2), 6.582 (s, 2H, H-6×2), 5.162 (s, 2H, CH₂), 4.790 (s, 2H, CH₂), 3.935 (s, 6H, 4-OCH₃×2), 3.781 (t, *J*=34.2Hz, 12H, 3-OCH₃, 5-OCH₃×2). LC-MS *m/z*: 578.28, calcd for C₃₂H₃₂FNO₈: 577.21.

1-isobutyryl-3,5-bis((E)-3,4,5-trimethoxybenzylidene)piperidin-4-one (13B): yellow powder, 43.6% yield, mp 152.6-156.0 °C. ¹H-NMR (CDCl₃) δ: 7.809 (d, *J*=33.0Hz, 2H, H-α×2), 6.744 (s, 2H, H-2×2), 6.636 (s, 2H, H-6×2), 4.971 (s, 2H, CH₂), 4.832 (s, 2H, CH₂), 3.937 (d, *J*=13.8 Hz, 18H, 3-OCH₃, 4-OCH₃, 5-OCH₃×2), 2.626-2.670 (m, 2H, CH₂), 1.043 (d, *J*=7.2Hz, 6H, CH₃×2). LC-MS *m/z*: 526.34, calcd for C₂₉H₃₅NO₈: 525.24.

4.1.2 Synthetic procedures

4.1.2.1 General synthetic procedure for the synthesis of **F35** and **F36**

4-piperidone hydrochloride hydrate **2** (5.0 mmol) and aryl aldehydes (10.0 mmol 3,4,5-trimethoxybenzaldehyde, 3,4-dimethoxybenzaldehyde) were dissolved in the mixture solvent of ethanol and water (10:1) and 40% NaOH aqueous solution was added into the solution to catalyze the reaction. The reaction stirred at room temperature for 12 h, the precipitate was formed. After filtration and washing with water and then recrystallized from ethanol to obtain desired products.

4.1.2.2. General synthetic procedure for the synthesis of **5B-13B**

NaH (60% dispersion in mineral oil, 2.0 mmol) was added in portions to a stirred solution of **F35** or **F36** (2.0 mmol) in anhydrous THF (10.0 mL) cooled in an ice bath. The resulting mixture was then allowed slowly to warm to room temperature. After stirring for 30 min, different alkyl halide or acyl chloride (3.0 mmol) in anhydrous THF (3.0 mL) was added drop wise. When TLC monitoring showed complete consumption of the starting material, the reaction mixture was evaporated under reduced pressure. The resulting solid was purified by silica gel chromatography using hexane and ethyl acetate gradient to obtain desired products.

4.2 Cells culture and MTT assay

Human lung cancer cell lines H460, A549, H1650, H1975 and normal human liver cell line HL7702 were all obtained from Chinese academy of sciences, a typical cell library culture preservation committee (China, shanghai). All cell lines were cultured in 1640 medium (Gibco, Eggenstein, Germany), which contained 10% heat-inactivated fetal bovine serum, 100 IU/mL penicillin and 100 µg/mL streptomycin, growing in the humidifying cultivating environment of 5% CO₂ at 37 °C.

The rate of cell viability was evaluated by 3-(4,5-dimethylthiazol-2-yl)-2,5-diphenyltetrazolium bromide (MTT) assay. In short, H460, A549, H1650, H1975 and HL7702 cells were seeded in 96-well plates with the cell density of 4000 per hole and left adherenced overnight. The various concentrations of compounds were then diluted in 1640 medium for three holes repeatability. The cell viability was detected after 72 h incubation with tested substances, drugs were acted in transfected cells for 24 h besides, 25 µL MTT (5 mg/mL) was then added per hole for 4 h at incubator,

DMSO dissolving crystallization, and the absorbance was detected at 490 nm by ELIASA.

4.3 Acute toxicity experiment

To assess the toxicity of the preferred compound, acute toxicity test was used. The C57BL/6 mice were purchased from SHANGHAI SLAC and observed for one week in a controlled environment (air-conditioning, $50 \pm 10\%$ relative humidity, $T = 22 \pm 2$ °C) prior to the experiments. The mice were then randomly assigned to different groups, respectively administered by intraperitoneal injection and lavage two ways to assess subjects compounds at a volume of 1 g/kg body weight. Solution of the compounds of intraperitoneal injection was prepared in 6% castor oil and gavage solvent was 0.5% CMC-Na. After more than ten days of continuous observation, the state and weight of the mice were recorded.

4.4 Cell cycle

2 mL A549 cell suspension (6×10^5) was vaccinated in the diameter of 60 mm Petri dishes and allowed to be cultured overnight. The cells were then incubated with compounds with prescribed concentrations for 10 h. All cells were harvested by digesting with trypsin and washed with PBS (Sigma-Aldrich, Germany) and then fixed with ice-cold 70% ethanol in PBS for 30 min at -20 °C. Fixed cells were washed with PBS, treated with RNase A (10 mg/mL) and resuspended in 50 µg/mL propidium iodide (PI) for staining. Cell cycle distribution was performed with FACSCalibur flow cytometer (BD Biosciences, CA).

4.5 Western blot

The cells were lysed in protein lysate buffer for 10 min. Total proteins were centrifuged at 12,000 rpm for 10 min at 4 °C and quantified. Protein samples were separated with 10% SDS-PAGE gel. After electrophoresis, the proteins in the gel were transferred to PVDF membrane, incubated with 5% skim milk for 1.5 h. After overnight incubation with the primary antibody, protein samples were incubated with HRP-conjugated secondary antibodies for 1 h. The results were detected by Quantity One software. The anti-p-IKK β , anti-IKK β , anti-I κ B α , anti-GAPDH, anti-Bax, anti-cleaved PARP, anti-p-JNK, anti-JNK, goat anti-rabbit IgG-HRP, goat anti-

mouse IgG-HRP antibodies were obtained from Santa Cruz Biotechnology (Santa Cruz, CA).

4.6 Apoptosis assay

For cell apoptosis analysis, after treatment for 24 h, cells were collected by the pancreatin without EDTA. In some experiments, NAC (5 mM) was pre-incubated for 1 h before the exposure of tested substances. Cells were stained with 3 μ L FITC Annexin V and 1 μ L PI for 15 min at room temperature avoiding light, and immediately analyzed on FACSCalibur flow cytometer (BD Biosciences, CA). The PI/RNase staining buffer was purchased from BD Bioscience (Franklin Lakes, NJ).

4.7 Hoechst 33258

A549 cells were inoculated in the Petri dishes of 3 cm diameter 1.2×10^6 cells per well overnight, then replaced liquid, added compounds with the prescribed concentrations. After 24 h drug action, the cells were fixed and stained by Hoechst 33258. The nuclear morphometry was observed by the fluorescence microscope. Under the magnification of 200, compounds could induce cell apoptosis obviously. Hoechst 33258 kit was obtained from Beyotime Institute of Biotechnology.

4.8 Determination of the level of ROS

The generation of ROS was detected by flow cytometry. A549 cells (6×10^5) were seeded in the diameter of 60 mm Petri dishes and exposed to 10 μ M of compound for different times or various concentrations for 9 h. In some experiments, NAC (5 mM) was pre-incubated for 1 h before the compounds exposure, and ROS levels were determined. Cells were incubated with DCF-DA (10 μ M) in the dark at 37 °C for 30 min. Then the cells were collected, washed in PBS and analyzed by flow cytometer.

4.9 Cell transfection

Cells were seeded in 6-well dishes at a density of 3×10^5 cells per well and cultured at 37 °C with 5% CO₂ overnight. Before transfection, cells were washed by PBS and added serum-free medium. Next, the mixture of high levels of plasmid and 2 μ L of lipofectamine 2000 as well as separate lipofectamine 2000 were added to the cell culture in each well respectively. After 6 h, the complex medium was removed and replaced by the 1640 medium contained 10% fetal bovine serum (FBS) and 1%

penicillin-streptomycin solution. After further incubated for 12 h, cells were rinsed twice with PBS, harvested by cell lysate and then detected by western blot.

4.10 Clonogenic assay

A549 cells were seeded in 6-well plates with the cell density of 1000 per hole and exposed to the absence or presence of drugs with various concentrations for holes respectively. Growth media with or without drugs was replaced after 2 days. And 8 days later, cells were fixed with methanol (1%) and formaldehyde (1%), stained with 0.5% crystal violet, then photographed by camera.

4.11 Statistical analysis

Data were expressed as means \pm SEM of three independent experiments. Student's t-test and two-way ANOVA were employed to analyze the statistical comparisons between sets of data. Significant differences were established at $P < 0.05$.

Acknowledgement

This work was supported by the ZheJiang Province Natural Science Fund of China (Grant Nos. LY17H160059), the National Natural Science Foundation of China (Grant Nos. 81703766, 81402839). The Opening Project of Zhejiang Provincial Top Key Discipline of Pharmaceutical Sciences.

References

- [1] B. Dholaria, W. Hammond, A. Shreders, Y. Lou, Emerging therapeutic agents for lung cancer, *Journal of Hematology & Oncology*, 9 (2016) 138-151.
- [2] A. Aggarwal, G. Lewison, S. Idir, M. Peters, C. Aldige, W. Boerckel, P. Boyle, E.L. Trimble, P. Roe, T. Sethi, J. Fox, R. Sullivan, The state of lung cancer research: a global analysis, *Journal of Thoracic Oncology: Official Publication of The International Association for The Study of Lung Cancer*, 11 (2016) 1040-1050.
- [3] F.R. Hirsch, G.V. Scagliotti, J.L. Mulshine, R. Kwon, W.J. Curran, Y.L. Wu, L. Paz-Ares, Lung cancer: current therapies and new targeted treatments, *The Lancet*, 389 (2017) 299-311.
- [4] D. Hardy, C.C. Liu, J.N. Cormier, R. Xia, X.L. Du, Cardiac toxicity in association with chemotherapy and radiation therapy in a large cohort of older patients with non-small-cell lung cancer, *Annals of Oncology: Official Journal of The European Society for Medical Oncology*, 21 (2010) 1825-1833.
- [5] N. Navani, M. Nankivell, D.R. Lawrence, S. Lock, H. Makker, D.R. Baldwin, R.J. Stephens, M.K. Parmar, S.G. Spiro, S. Morris, S.M. Janes, Lung cancer diagnosis and staging with

- endobronchial ultrasound-guided transbronchial needle aspiration compared with conventional approaches: an open-label, pragmatic, randomised controlled trial, *The Lancet Respiratory Medicine*, 3 (2015) 282-289.
- [6] S.L. Wood, M. Pernemalm, P.A. Crosbie, A.D. Whetton, Molecular histology of lung cancer: from targets to treatments, *Cancer Treatment Reviews*, 41 (2015) 361-375.
- [7] A. Hill, D. Gotham, J. Fortunak, J. Meldrum, I. Erbacher, M. Martin, H. Shoman, J. Levi, W.G. Powderly, M. Bower, Target prices for mass production of tyrosine kinase inhibitors for global cancer treatment, *BMJ Open*, 6 (2016) e009586-e009594.
- [8] Z. MF, Analytic inquiry: molecular testing in lung cancer, *Cancer Cytopathology*, 125 (2017) 470-476.
- [9] J.M. Sun, D.W. Hwang, J.S. Ahn, M.J. Ahn, K. Park, Prognostic and predictive value of KRAS mutations in advanced non-small cell lung cancer, *Plos One*, 8 (2013) e64816-e64823.
- [10] C. Gridelli, P.C. Sacco, Novel cytotoxic drugs in advanced nonsmall cell lung cancer, *Current Opinion in Oncology*, 28 (2016) 110-114.
- [11] B.H. Gronberg, S. Sundstrom, S. Kaasa, R.M. Bremnes, O. Flotten, T. Amundsen, H.H. Hjelde, C. Plessen, M. Jordhoy, Influence of comorbidity on survival, toxicity and health-related quality of life in patients with advanced non-small-cell lung cancer receiving platinum-doublet chemotherapy, *European Journal of Cancer*, 46 (2010) 2225-2234.
- [12] S. Heavey, P. Godwin, A.M. Baird, M.P. Barr, K. Umezawa, S. Cuffe, S.P. Finn, K.J. O'Byrne, K. Gately, Strategic targeting of the PI3K-NF κ B axis in cisplatin-resistant NSCLC, *Cancer Biology & Therapy*, 15 (2014) 1367-1377.
- [13] L. Yang, Y. Zhou, Y. Li, J. Zhou, Y. Wu, Y. Cui, G. Yang, Y. Hong, Mutations of p53 and KRAS activate NF- κ B to promote chemoresistance and tumorigenesis via dysregulation of cell cycle and suppression of apoptosis in lung cancer cells, *Cancer Letters*, 357 (2015) 520-526.
- [14] P.V.S. Ramya, L. Guntuku, S. Angapelly, C.S. Digwal, U.J. Lakshmi, D.K. Sigalapalli, B.N. Babu, V.G.M. Naidu, A. Kamal, Synthesis and biological evaluation of curcumin inspired imidazo[1,2-a]pyridine analogues as tubulin polymerization inhibitors, *European Journal of Medicinal Chemistry*, 143 (2017) 216-231.
- [15] R. Wilken, M.S. Veena, M.B. Wang, E.S. Srivatsan, Curcumin: a review of anti-cancer properties and therapeutic activity in head and neck squamous cell carcinoma, *Molecular Cancer*, 10 (2011) 12-30.
- [16] R.I. Mahran, M.M. Hagra, D. Sun, D.E. Brenner, Bringing curcumin to the clinic in cancer prevention: a review of strategies to enhance bioavailability and efficacy, *The American Association of Pharmaceutical Scientists Journal*, 19 (2017) 54-81.
- [17] C. Zhao, Z. Liu, G. Liang, Promising curcumin-based drug design: mono-carbonyl analogues of curcumin (MACs), *Current Pharmaceutical Design*, 19 (2013) 2114-2135.
- [18] Q. Weng, L. Fu, G. Chen, J. Hui, J. Song, J. Feng, D. Shi, Y. Cai, J. Ji, G. Liang, Design, synthesis, and anticancer evaluation of long-chain alkoxyated mono-carbonyl analogues of curcumin, *European Journal of Medicinal Chemistry*, 103 (2015) 44-55.
- [19] G. Liang, H. Zhou, Y. Wang, E.C. Gurley, B. Feng, L. Chen, J. Xiao, S. Yang, X. Li, Inhibition of LPS-induced production of inflammatory factors in the macrophages by mono-carbonyl analogues of curcumin, *Journal of Cellular and Molecular Medicine*, 13 (2009) 3370-3379.

- [20] C. Zhao, Y. Cai, X. He, J. Li, L. Zhang, J. Wu, Y. Zhao, S. Yang, X. Li, W. Li, G. Liang, Synthesis and anti-inflammatory evaluation of novel mono-carbonyl analogues of curcumin in LPS-stimulated RAW 264.7 macrophages, *European Journal of Medicinal Chemistry*, 45 (2010) 5773-5780.
- [21] F. Schmitt, M. Gold, G. Begemann, I. Andronache, B. Biersack, R. Schobert, Fluoro and pentafluorothio analogs of the antitumoral curcuminoid EF24 with superior antiangiogenic and vascular-disruptive effects, *Bioorganic & Medicinal Chemistry*, 25 (2017) 4894-4903.
- [22] S. Bisht, M. Schlesinger, A. Rupp, R. Schubert, J. Nolting, J. Wenzel, S. Holdenrieder, P. Brossart, G. Bendas, G. Feldmann, A liposomal formulation of the synthetic curcumin analog EF24 (Lipo-EF24) inhibits pancreatic cancer progression: towards future combination therapies, *Journal of Nanobiotechnology*, 14 (2016) 57-71.
- [23] H.I. Onen, A. Yilmaz, E. Alp, A. Celik, S.M. Demiroz, E. Konac, I.C. Kurul, E.S. Menevse, EF24 and RAD001 potentiates the anticancer effect of platinum-based agents in human malignant pleural mesothelioma (MSTO-211H) cells and protects nonmalignant mesothelial (MET-5A) cells, *Human & Experimental Toxicology*, 34 (2015) 117-126.
- [24] J. Wu, Y. Zhang, Y. Cai, J. Wang, B. Weng, Q. Tang, X. Chen, Z. Pan, G. Liang, S. Yang, Discovery and evaluation of piperid-4-one-containing mono-carbonyl analogs of curcumin as anti-inflammatory agents, *Bioorganic & Medicinal Chemistry*, 21 (2013) 3058-3065.
- [25] P. Qiu, S. Zhang, Y. Zhou, M. Zhu, Y. Kang, D. Chen, J. Wang, P. Zhou, W. Li, Q. Xu, R. Jin, J. Wu, G. Liang, Synthesis and evaluation of asymmetric curcuminoid analogs as potential anticancer agents that downregulate NF- κ B activation and enhance the sensitivity of gastric cancer cell lines to irinotecan chemotherapy, *European Journal of Medicinal Chemistry*, 139 (2017) 917-925.
- [26] Y. Xia, B. Weng, Z. Wang, Y. Kang, L. Shi, G. Huang, S. Ying, X. Du, Q. Chen, R. Jin, J. Wu, G. Liang, W346 inhibits cell growth, invasion, induces cycle arrest and potentiates apoptosis in human gastric cancer cells in vitro through the NF- κ B signaling pathway, *Tumour Biology: The Journal of The International Society for Oncodevelopmental Biology and Medicine*, 37 (2016) 4791-4801.
- [27] S. Ying, X. Du, W. Fu, D. Yun, L. Chen, Y. Cai, Q. Xu, J. Wu, W. Li, G. Liang, Synthesis, biological evaluation, QSAR and molecular dynamics simulation studies of potential fibroblast growth factor receptor 1 inhibitors for the treatment of gastric cancer, *European Journal of Medicinal Chemistry*, 127 (2017) 885-899.
- [28] Y. Wang, J. Chang, X. Liu, X. Zhang, S. Zhang, X. Zhang, D. Zhou, G. Zheng, Discovery of piperlongumine as a potential novel lead for the development of senolytic agents, *Aging*, 8 (2016) 2915-2926.
- [29] H. Chen, Y. Li, C. Sheng, Z. Lv, G. Dong, T. Wang, J. Liu, M. Zhang, L. Li, T. Zhang, D. Geng, C. Niu, K. Li, Design and synthesis of cyclopropylamide analogues of combretastatin-A4 as novel microtubule-stabilizing agents, *Journal of Medicinal Chemistry*, 56 (2013) 685-699.
- [30] M. Fulciniti, N. Amodio, R.L. Bandi, M. Munshi, G. Yang, L. Xu, Z. Hunter, P. Tassone, K. C. Anderson, S.P. Treon, N.C. Munshi, MYD88-independent growth and survival effects of Sp1 transactivation in Waldenström macroglobulinemia, *Blood*, 123 (2014) 2673-2681.
- [31] K.M. Terlikowska, A.M. Witkowska, M.E. Zujko, B. Dobrzycka, S.J. Terlikowski, Potential application of curcumin and its analogues in the treatment strategy of patients with primary

- epithelial ovarian cancer, *International Journal of Molecular Sciences*, 15 (2014) 21703-21722.
- [32] T. Kalai, M.L. Kuppusamy, M. Balog, K. Selvendiran, B.K. Rivera, P. Kuppusamy, K. Hideg, Synthesis of N-substituted 3,5-bis(arylidene)-4-piperidones with high antitumor and antioxidant activity, *Journal of Medicinal Chemistry*, 54 (2011) 5414-5421.
- [33] E. Grella, A. Ząbek, A. Grabowiecka, Interferences in the optimization of the MTT assay for viability estimation of proteus mirabilis, *Avicenna Journal Medical Biotechnol*, 7 (2015) 159-167.
- [34] M.C. Araujo, N.M. Barcellos, P.M. Vieira, T.M. Gouveia, M.O. Guerra, V.M. Peters, D.A. Saude-Guimaraes, Acute and sub chronic toxicity study of aqueous extract from the leaves and branches of *Campomanesia velutina* (Cambess) O. Berg, *Journal of Ethnopharmacology*, 201 (2017) 17-25.
- [35] S. Prasad, S.C. Gupta, A.K. Tyagi, Reactive oxygen species (ROS) and cancer: role of antioxidative nutraceuticals, *Cancer Letters*, 387 (2017) 95-105.
- [36] J.N. Moloney, T.G. Cotter, ROS signalling in the biology of cancer, *Seminars in Cell & Developmental Biology*, (2017), doi.org/10.1016/j.semcdb.2017.05.023.
- [37] A.T. Dharmaraja, Role of reactive oxygen species (ROS) in therapeutics and drug resistance in cancer and bacteria, *Journal of Medicinal Chemistry*, 60 (2017) 3221-3240.
- [38] C. Feng, Y. Xia, P. Zou, M. Shen, J. Hu, S. Ying, J. Pan, Z. Liu, X. Dai, W. Zhuge, G. Liang, Y. Ruan, Curcumin analog L48H37 induces apoptosis through ROS-mediated endoplasmic reticulum stress and STAT3 pathways in human lung cancer cells, *Molecular Carcinogenesis*, 56 (2017) 1765-1777.
- [39] X. Zhang, M. Chen, P. Zou, K. Kanchana, Q. Weng, W. Chen, P. Zhong, J. Ji, H. Zhou, L. He, G. Liang, Curcumin analog WZ35 induced cell death via ROS-dependent ER stress and G2/M cell cycle arrest in human prostate cancer cells, *BioMed Central Cancer*, 15 (2015) 866-876.
- [40] G. He, C. Feng, R. Vinothkumar, W. Chen, X. Dai, X. Chen, Q. Ye, C. Qiu, H. Zhou, Y. Wang, G. Liang, Y. Xie, W. Wu, Curcumin analog EF24 induces apoptosis via ROS-dependent mitochondrial dysfunction in human colorectal cancer cells, *Cancer Chemotherapy and Pharmacology*, 78 (2016) 1151-1161.
- [41] T. Liang, X. Zhang, W. Xue, S. Zhao, X. Zhang, J. Pei, Curcumin induced human gastric cancer BGC-823 cells apoptosis by ROS-mediated ASK1-MKK4-JNK stress signaling pathway, *International Journal of Molecular Sciences*, 15 (2014) 15754-15765.
- [42] W. Chen, P. Zou, Z. Zhao, X. Chen, X. Fan, R. Vinothkumar, R. Cui, F. Wu, Q. Zhang, G. Liang, J. Ji, Synergistic antitumor activity of rapamycin and EF24 via increasing ROS for the treatment of gastric cancer, *Redox Biology*, 10 (2016) 78-89.
- [43] S.J. Chen, S.S. Huang, N.S. Chang, Role of WWOX and NF- κ B in lung cancer progression, *Translational Respiratory Medicine*, 1 (2013) 1-10.
- [44] W. Chen, Z. Li, L. Bai, Y. Lin, NF-kappaB, a mediator for lung carcinogenesis and a target for lung cancer prevention and therapy, *Frontiers in Bioscience A Journal & Virtual Library*, 16 (2012) 1172-1185.
- [45] A.L. Kasinski, Y. Du, S.L. Thomas, J. Zhao, S.Y. Sun, F.R. Khuri, C.Y. Wang, M. Shoji, A. Sun, J.P. Snyder, D. Liotta, H. Fu, Inhibition of IkappaB kinase-nuclear factor-kappaB signaling pathway by 3,5-bis(2-fluorobenzylidene)piperidin-4-one (EF24), a novel

- monoketone analog of curcumin, *Molecular Pharmacology*, 74 (2008) 654-661.
- [46] Y.M. Ma, Y.M. Peng, Q.H. Zhu, A.H. Gao, B. Chao, Q.J. He, J. Li, Y.H. Hu, Y.B. Zhou, Novel CHOP activator LGH00168 induces necroptosis in A549 human lung cancer cells via ROS-mediated ER stress and NF- κ B inhibition, *Acta Pharmacologica Sinica*, 37 (2016) 1381-1390.
- [47] P. Zhang, J. Chen, Y. Wang, Y. Huang, Y. Tian, Z. Zhang, F. Xu, Discovery of potential biomarkers with dose- and time-dependence in cisplatin-induced nephrotoxicity using metabolomics integrated with a principal component-based area calculation strategy, *Chemical Research in Toxicology*, 29 (2016) 776-783.
- [48] B. Insuasty, D. Becerra, J. Quiroga, R. Abonia, M. Nogueras, J. Cobo, Microwave-assisted synthesis of pyrimido[4,5-b][1,6]naphthyridin-4(3H)-ones with potential antitumor activity, *European Journal of Medicinal Chemistry*, 60 (2013) 1-9.

Highlights

- A series of EF24 analogues with cytotoxic activities selectively towards lung cancer cells were designed and synthesized. **5B** showed lower toxicity than EF24 both *in vitro* and *vivo*.
- **5B** could significantly enhance the sensitivity of A549 cells to cisplatin or 5-Fu.
- **5B** exerted anti-tumor activities by activating JNK and inhibiting NF- κ B signaling pathways respectively, both of which were associated with the generation of ROS.